

July 2025

“Testing mean densities with an application to climate
change in Vietnam”

Camille Mondon, Thi-Huong Trinh, Josep Antoni Martín-Fernández
and Christine Thomas-Agnan

Testing mean densities with an application to climate change in Vietnam

July 1, 2025

Camille Mondon^{1*}, Huong Thi Trinh², Josep Antoni Martín-Fernández³,
Christine Thomas-Agnan⁴

^{1*}Faculty of Mathematical Economics, Thuongmai University, Ho Tung Mau street, Hanoi, 10000, Vietnam.

²Toulouse School of Economics, University of Toulouse Capitole, Toulouse, 31000, France.

³Department IMAE, Universitat de Girona, Campus Montilivi. Edifici P4. Carrer Maria Aurèlia Capmany i Farnés, 61, Girona, E-17003, Spain.

*Corresponding author(s). E-mail(s): camille.mondon@tse-fr.eu;
Contributing authors: trinhthihuong@tmu.edu.vn; josepantoni.martin@udg.edu;
christine.thomas@tse-fr.eu;

Abstract

Given samples of density functions on an interval (\mathbf{a}, \mathbf{b}) of \mathbb{R} , categorized according to a factor variable, we aim to test the equality of their mean functions both overall and across the groups defined by the factor. While the Functional Analysis of Variance (FANOVA) methodology is well-established for functional data, its adaptation to density functions (DANOVA) is necessary due to their inherent constraints of positivity and unit integral. To accommodate these constraints, we naturally use Bayes spaces methodology by mapping the densities using the centered log-ratio transformation into the $L_0^2(\mathbf{a}, \mathbf{b})$ space where we can use FANOVA techniques. Many traditional contrasts in FANOVA rely on squared differences and can be reinterpreted as squared distances between Bayes perturbations within the densities space. We illustrate our methodology on a dataset comprising daily maximum temperatures across Vietnamese provinces between 1987 and 2016. Within the context of climate change, we first investigate the existence of a non-zero temporal trend of the densities of daily maximum temperature over Vietnam and then examine whether there is any regional effect on these trends. Finally, we explore odds ratio based interpretations allowing to describe the trends more locally.

Keywords: Analysis of variance, Density data, Functional data, Log ratio, Odds ratio, Bayes spaces

1 Introduction

Climate change remains a central focus of scientific inquiry, as its effects on weather patterns, ecosystems, and human livelihoods become increasingly pronounced (Hultgren et al., 2022). According to the World Meteorological Organization, the global mean temperature during the 2011–2020 period has been $1.10 \pm 0.12^\circ\text{C}$ higher than the average recorded between 1850 and

1900. Notably, weather-related events accounted for nearly 94% of all recorded disaster-induced displacements over the past decade (World Meteorological Organization, 2023). Among the various global climate indicators, near-surface temperature is particularly critical, as it directly influences human well-being and daily activities (Gubler et al., 2023; World Meteorological Organization, 2024; Schlenker and Roberts, 2009). Temperatures can be measured using various

20 indicators, such as heat stress, growing degree
21 days, killing degree days, temperature intervals,
22 or the entire temperature distribution (Roberts
23 et al., 2013; Vo et al., 2022; Espagne et al., 2019;
24 Schlenker and Roberts, 2009; Hultgren et al.,
25 2022). Indeed, considering the entire temperature
26 distribution captures the full range of temper-
27 atures throughout each day and over multiple
28 days, offering a more comprehensive and infor-
29 mative perspective (Hsiang et al., 2017; Trinh
30 et al., 2023). Vietnam lies closer to the tropics
31 than the equator and is significantly influenced
32 by the East Sea, resulting in a predominantly
33 tropical monsoon climate. The country’s econ-
34 omy is heavily reliant on agriculture, supported
35 by its fertile deltas, mountainous regions, and
36 extensive coastline. Vietnam has been identified
37 as one of the five countries most vulnerable to the
38 impacts of climate change (World Bank Group
39 and Asian Development Bank, 2021; Trinh et al.,
40 2021). Since 1960, the country’s mean annual
41 temperature has risen by approximately 0.5°C
42 to 0.7°C, with an estimated warming rate of
43 0.26°C per decade between 1971 and 2010 (World
44 Bank Group and Asian Development Bank, 2021).
45 Consequently, as in many other nations, analyz-
46 ing climate change in Vietnam is of particular
47 interest due to its significant implications for
48 agriculture, especially rice cultivation (Tran and
49 Nguyen, 2021; Trinh et al., 2021; Trinh, 2018)

50 With the increasing volume of recorded data,
51 data science has seen the rise of new types
52 of observations like functional data. Functional
53 data analysis is currently a very active field of
54 statistics, see Aneiros et al. (2022). Of particu-
55 lar interest for our application are density-valued
56 data, which can be found in other areas of social
57 sciences (for example age distributions, income
58 distributions, expenditure distributions), and in
59 other fields (for example particle size distribu-
60 tions). Density data require a specific treatment
61 within the framework of functional data anal-
62 ysis, due to their inherent constraints, namely
63 non-negativity and integration to one. It is typi-
64 cally assumed that each observation corresponds
65 to a sampled continuous density function, belong-
66 ing to an infinite-dimensional function space, as
67 discussed in Petersen et al. (2022). A smooth-
68 ing tool is necessary to fill the gap between the
69 discrete data and the continuous temperature
70 density objects and this procedure step is called
71 preprocessing. Among the methods described in
72 Petersen et al. (2022), we use the Bayes spaces
73 approach first introduced in Egozcue et al. (2006),

74 and later on developed in Van Den Boogaart et al.
75 (2010, 2014).

76 In this paper, we focus on testing mean den-
77 sity functions, investigating their equality to a
78 reference density as well as their equality across
79 groups. Since density functions share similar con-
80 straints with compositional vectors, albeit in a
81 continuous form, we build upon techniques from
82 compositional data analysis (CoDA) but also from
83 the functional analysis of variance (FANOVA)
84 framework, introduced in Ramsay and Silverman
85 (2005); Kokoszka and Reimherr (2017).

86 Before comparing group means, a first ques-
87 tion can be to find whether the expected density
88 is equal to a given reference, for example the uni-
89 form density. We adapt the one-sample test from
90 the functional framework (see Zhang (2013)) to
91 density functions in Section 4.1.

92 As outlined by Martín-Fernández et al. (2015),
93 the analysis of grouped data typically begins
94 with testing the equality of group means and a
95 widely used approach for this purpose in CoDA is
96 the multivariate analysis of variance (MANOVA)
97 contrast, which needs to be adapted here to con-
98 tinuous objects. On the other hand, the FANOVA
99 techniques must be adapted when applied to
100 density functions because they reside in the con-
101 strained space $B^2(a, b)$. We present five test
102 statistics in Section 4.2 for the problem of testing
103 the equality of group means of density functions,
104 which we call DANOVA for distributional analysis
105 of variance.

106 When an ANOVA test leads to a rejection
107 of the null hypothesis of equal group means,
108 a related question of interest is the pairwise
109 comparison of group means (see for example
110 Martín-Fernández et al., 2015, who present addi-
111 tional techniques for interpreting the differences
112 between the groups in CoDA). This question is
113 treated in Section 4.3.

114 Finally, to go beyond the global comparisons
115 of densities and do a more local analysis, we adapt
116 a technique based on odds ratios from Maier et al.
117 (2025) to infer the relative mass of the densities
118 over specific intervals.

119 We apply the above tools to address different
120 questions relative to climate change in Vietnam.
121 We use the distributions of maximum temper-
122 atures in the provinces of Vietnam to compare
123 the six administrative regions in terms of cli-
124 mate change. The dataset and its preprocessing
125 are presented in Section 3. After constructing a
126 trend slope density for each province summariz-
127 ing its time evolution, we investigate maximum
128 temperature distribution changes through these

129 trend slope densities sample. A one-sample test
 130 comparing the mean slope density to the uniform
 131 distribution addresses the question of the exist-
 132 ence of a climate change in the whole of Vietnam
 133 in Section 4.1. Then, an analysis of variance of the
 134 slope densities in Section 4.2 detects whether the
 135 climate change is the same across regions. Finally
 136 in Section 5, we compare the relative frequencies
 137 in different subintervals of the temperature distri-
 138 bution using infinitesimal odds ratios introduced
 139 in Maier et al. (2025).

140 2 Framework and reminders

141 2.1 Reminders on functional 142 analysis of variance

143 In the classical framework of Functional Analysis
 144 of Variance, or simply FANOVA (as presented in
 145 Zhang, 2013, p. 144), we observe G independent
 146 functional samples, denoted by $(f_{g1}, \dots, f_{gn_g})$ for
 147 $1 \leq g \leq G$, from stochastic processes with values
 148 in $L^2(a, b)$, satisfying for $1 \leq i \leq n_g$ and $a \leq x \leq$
 149 b

$$181 f_{gi}(x) = f_g(x) + v_{gi}(x), \quad (1)$$

150 where $f_g(x) = \mathbb{E}(f_{gi})(x)$ is the unknown mean
 151 function in group g and the stochastic error pro-
 152 cess v_{gi} has mean 0 and common covariance
 153 operator. The total sample size is $n = \sum_{g=1}^G n_g$.
 154 The overall sample mean curve $\bar{f}_{..}$ and the group
 155 sample mean curves \bar{f}_g are respectively defined
 156 by

$$182 \bar{f}_{..}(x) = \frac{1}{n} \sum_{g=1}^G \sum_{i=1}^{n_g} f_{gi}(x) \quad (2)$$

$$183 \bar{f}_g(x) = \frac{1}{n_g} \sum_{i=1}^{n_g} f_{gi}(x) \quad (3)$$

157 The pointwise between-group mean square error
 158 and the pointwise within-group mean square error
 159 at x are respectively defined by

$$184 \text{SSB}(x) = \sum_{g=1}^G n_g (\bar{f}_g(x) - \bar{f}_{..}(x))^2 \text{ and} \quad (4)$$

$$185 \text{SSW}(x) = \sum_{g=1}^G \sum_{i=1}^{n_g} (f_{gi}(x) - \bar{f}_g(x))^2. \quad (5)$$

160 Ramsay and Silverman (2005) extend the classical
 161 F-test and propose the pointwise functional F-
 162 ratio to test the equality of the group mean curves

at a given point x , using the local F-statistic

$$163 F(x) = \frac{\text{SSB}(x)}{\text{SSW}(x)}. \quad (6)$$

164 For a global assessment of the equality of the
 165 group mean curves on the whole interval of vari-
 166 ation of their argument, Zhang and Chen (2007)
 167 and Zhang (2013) introduce L^2 -norm based tests
 168 as well as F-type test statistics. Later on, Zhang
 169 and Liang (2014) propose the GPF test based on
 170 the integral of the pointwise F-ratio statistic and
 171 the F_{\max} test based on the maximum of the point-
 172 wise F-test. It is then necessary to approximate
 173 the null distribution of these statistics. This can
 174 be achieved using a permutation based procedure
 175 as in Ramsay and Silverman (2005) or a bootstrap
 176 procedure as in Zhang et al. (2019).

177 2.2 Reminders on distributional 178 data analysis and Bayes spaces

179 Egozcue et al. (2006) and Van Den Boogaart et al.
 180 (2010, 2014) define the Bayes spaces of prob-
 181 ability density functions relative to a reference
 182 measure λ on an interval of \mathbb{R} , in a similar fash-
 183 ion as $L^2(\lambda)$ spaces. In the following, the measure
 184 λ will be Lebesgue measure on a finite interval
 185 $[a, b]$ and we will denote these spaces by $B^2(a, b)$.
 186 We consider the separable Hilbert space $L_0^2(a, b)$
 187 of square-integrable functions with a zero inte-
 188 gral on (a, b) equipped with the inner product
 189 $\langle f, g \rangle_{L^2} = \int_a^b fg \, d\lambda$. For any measurable function
 190 $p : [a, b] \rightarrow \mathbb{R}$ that is positive almost everywhere
 191 and such that the function $\log(p)$ is integrable, we
 192 can define its centered log-ratio transform $\text{clr}(p)$

$$193 x \in [a, b] \mapsto \log(p(x)) - \frac{1}{b-a} \int_a^b \log(p)(u) du. \quad (7)$$

194 Note that by construction $\text{clr}(p) \in L_0^2(a, b)$. Con-
 195 versely for each $f \in L_0^2(\lambda)$, the equivalence class
 196 $\text{clr}^{-1}(f) = \{\alpha \exp(f), \alpha > 0\}$ contains positive
 197 functions that are equal almost everywhere, up to
 198 a multiplicative constant. Among them there is a
 199 unique probability density function p (thus sat-
 200 isfying $\int_a^b p(u) \, du = 1$) that we use to represent
 201 $\text{clr}^{-1}(f)$.

202 Then the Bayes Hilbert space with Lebesgue
 203 reference measure on the interval $[a, b]$ is the set
 of probability density functions

$$204 B^2(a, b) = \{\text{clr}^{-1}(f), f \in L_0^2(a, b)\} \quad (8)$$

205 equipped with the only separable Hilbert
 space structure $(\oplus, \odot, \langle \cdot, \cdot \rangle_{B^2})$ that makes

206 the centered log-ratio transform an isometry 233
 207 between $(B^2(a, b), \oplus, \odot, \langle \cdot, \cdot \rangle_{B^2})$ and
 208 $(L_0^2(a, b), +, \cdot, \langle \cdot, \cdot \rangle_{L^2})$. The resulting addition
 209 \oplus is called Aitchison perturbation (\ominus denoting
 210 the negative perturbation) and the scalar
 211 multiplication \odot is called Aitchison powering.

212 Following Van Den Boogaart et al. (2014), it
 213 is also possible to use the centered log-ratio transform
 214 in order to transport to $B^2(a, b)$ the Borel
 215 sets, as well as the expectation and covariance of
 216 $L_0^2(a, b)$ -valued random variables. For a random
 217 density π in $B^2(a, b)$, one can define the expected
 218 value in the Bayes space:

$$\mathbb{E}^B(\pi) = \text{clr}^{-1}(\mathbb{E}[\text{clr}(\pi)]) \quad (9)$$

219 and the covariance operator, for $\phi \in B^2(a, b)$:

$$\begin{aligned} \text{Cov}^B[\pi](\phi) &= \text{clr}^{-1}(\text{Cov}^B[\text{clr} \pi](\text{clr} \phi)) = \\ \mathbb{E}^B [\langle \pi \ominus \mathbb{E}^B(\pi), \phi \rangle_{B^2} \odot (\pi \ominus \mathbb{E}^B(\pi))] &. \end{aligned} \quad (10)$$

220 *Notations for distributional analysis of* 221 *variance in Bayes spaces*

222 In order to avoid confusion, we adopt a specific
 223 notation to distinguish ordinary (unconstrained)
 224 functions from densities in a Bayes space. We
 225 observe G independent density samples, denoted
 226 by $(\pi_{g1}, \dots, \pi_{gn_g})$ for $1 \leq g \leq G$, from stochastic
 227 processes with values in $B^2(a, b)$, satisfying for
 228 $1 \leq i \leq n_g$ and $a \leq x \leq b$

$$\pi_{gi}(x) = (\pi_g \oplus u_{gi})(x), \quad (11)$$

229 where $\pi_g(x) = \mathbb{E}^B(\pi_{gi})(x)$ is the unknown mean
 230 density in group g and the stochastic error process
 231 u_{gi} has mean equal to the uniform distribution on
 232 (a, b) and common covariance operator (defined
 233 by (10) in Bayes spaces). The total sample size is
 234 $n = \sum_{g=1}^G n_g$. As above the overall sample mean
 235 density is defined as

$$\bar{\pi}_{..}(x) = \frac{1}{n} \odot \bigoplus_{g=1}^G \bigoplus_{i=1}^{n_g} \pi_{gi}(x)$$

and the sample mean density in group g as

$$\bar{\pi}_{g.}(x) = \frac{1}{n_g} \odot \bigoplus_{i=1}^{n_g} \pi_{gi}(x).$$

229 Applying the FANOVA formulas to the clr-
 230 transformed densities, we adapt the FANOVA
 231 framework to densities and define the point-
 232 wise between-group mean square error and the

pointwise within-group mean square error at x by

$$\text{SSB}(x) = \sum_{g=1}^G n_g (\text{clr}(\bar{\pi}_{g.})(x) - \text{clr}(\bar{\pi}_{..})(x))^2 \quad (12)$$

$$\text{SSW}(x) = \sum_{g=1}^G \sum_{i=1}^{n_g} (\text{clr}(\pi_{gi})(x) - \text{clr}(\bar{\pi}_{g.})(x))^2 \quad (13)$$

3 Data description and preprocessing

3.1 Description

237 The climate data used in this study comprises
 238 daily temperatures and precipitation, sourced
 239 from the Climate Prediction Center (CPC)
 240 database, developed by the National Oceanic and
 241 Atmospheric Administration (NOAA). This data
 242 provides historical records of the maximum and
 243 minimum temperatures for a 0.5-degree by 0.5-
 244 degree grid of latitude and longitude. For this
 245 study, we focus exclusively on maximum temper-
 246 atures as they are a direct indicator of heat stress
 247 on both humans and the environment. The data
 248 spans the years 1987 to 2016. In order to address
 249 the discrepancy between the geographical coordi-
 250 nates and the municipalities of Vietnam (63
 251 provinces), we calculate the average of all grid
 252 cells or the value of the four nearest localities to
 253 impute the missing data. This process results in
 254 365 or 366 daily maximum temperature records
 255 for each province and year.

256 During the study period, maximum tempera-
 257 tures (hereafter denoted T_{\max}) range from -5°C to
 258 nearly 45°C . However, extreme cold and extreme
 259 heat are rare. For the purpose of our analy-
 260 sis, we focus on a temperature range of 12°C
 261 to 40°C . Temperatures below 12°C are adjusted
 262 upward to 12°C , while temperatures exceeding
 263 40°C are capped at 40°C . As we can see on
 264 Figure 1, there are $n = 63$ provinces in Vietnam
 265 grouped into $G = 6$ socioeconomic regions. We
 266 use the following acronyms for the regions: NMM
 267 for Northern Midlands and Mountains region
 268 ($n_1 = 14$ provinces), RRD for Red River Delta
 269 region ($n_2 = 12$ provinces), NCC for North Cen-
 270 tral Coast region ($n_3 = 13$ provinces), CHR for
 271 Central Highlands region ($n_4 = 5$ provinces),
 272 SR for Southeast region ($n_5 = 6$ provinces)
 273 and MDR for Mekong Delta region ($n_6 = 13$
 274 provinces). Trinh et al. (2021) highlight the fact
 275 that the regions have their own weather peculiari-
 276 ties. Some regions in the north have four seasons:

277 winter, spring, summer, and autumn, while some 294
 278 regions in the south experience two distinct seasons: the dry season (November to April) and 295
 279 the rainy season (May to October) (Trinh et al., 296
 280 the rainy season (May to October) (Trinh et al., 297
 281 2021; World Bank Group and Asian Development 298
 282 Bank, 2021). For example, according to Trinh 299
 283 et al. (2021), during the period 1960-2000 winter 300
 284 temperatures rose faster than those of the summer, 301
 285 and temperatures in the northern zones rose 302
 faster than in the southern zones. 303

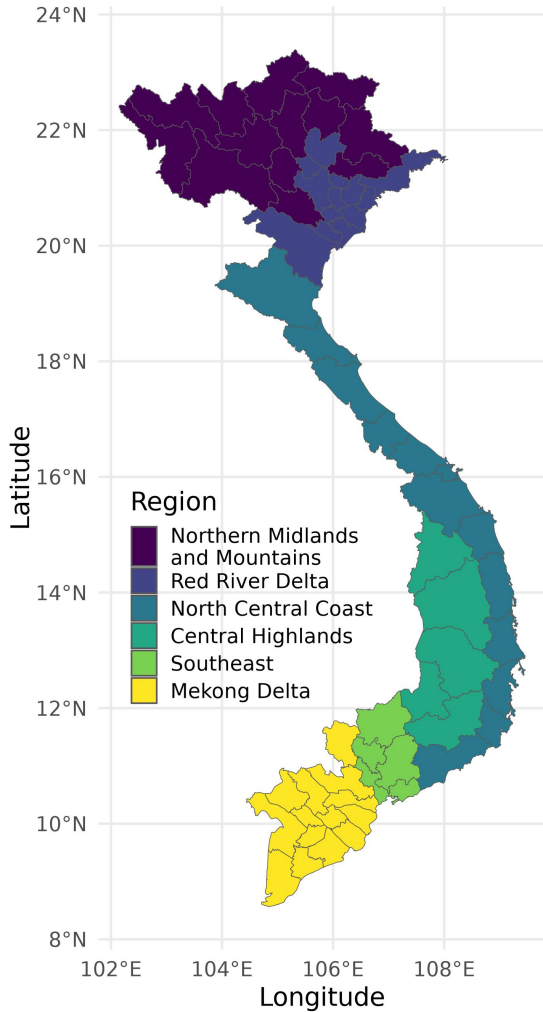


Fig. 1 Map of the provinces of Vietnam colored by region.

3.2 Smoothing

We will assume that the observed data arise from random densities, themselves sampled from an hypothesized and unknown distribution on a Bayes space. Since the elements of the Bayes spaces are density functions, whereas the observed data (usually samples of real-valued observations

or histograms) is always discrete, a preprocessing step is necessary to transform the observed samples or histograms into a sample of probability density functions. We will follow the preprocessing procedure of Machalová et al. (2016, 2021) to transform our yearly samples of maximum temperatures at the province level into density functions that belong to a finite-dimensional subspace $\mathcal{C}_d^\Delta(a, b)$ of the Bayes Hilbert space $B^2(a, b)$, made of compositional splines. A compositional spline (CB-spline) is a probability density function whose logarithm is a polynomial spline.

The process starts by the choice of a basis of normalized B-spline functions for the space $\mathcal{S}_d^\Delta(a, b) \subset L^2(a, b)$, of polynomial splines or order d (degree less than or equal to $d - 1$) and inside knots $\Delta = (\delta_1, \dots, \delta_k)$, of dimension $d + k$ (see Schumaker, 1981, for a complete description). To accommodate the zero-integral constraint, Machalová et al. (2016) introduce the ZB-spline functions, denoted by $Z_\ell(x), 1 \leq \ell \leq d + k - 1$ for the subspace $\mathcal{Z}_d^\Delta(a, b) = \mathcal{S}_d^\Delta(a, b) \cap L_0^2(a, b)$ of dimension $d + k - 1$, the loss of one dimension being due to the zero-integral constraint. Finally the inverse clr of the ZB-spline basis functions, called the CB-spline basis functions, denoted by $C_\ell = \text{clr}^{-1}(Z_\ell)$ generate the space $\mathcal{C}_d^\Delta(a, b)$, an Euclidean subspace of $B^2(a, b)$ of dimension $k + d - 1$, made of compositional splines on $[a, b]$ of order d with knots sequence Δ . The expansion (14) of a density π of the subspace $\mathcal{C}_d^\Delta(a, b)$ of $B^2(a, b)$ and the corresponding expansion (15) of its clr transform in the corresponding ZB-spline basis generating the space $\mathcal{Z}_d^\Delta(a, b)$ are then given by:

$$\pi(x) = \bigoplus_{\ell=1}^{d+k-1} [\pi]^{C_\ell} \odot C_\ell(x), \quad (14)$$

$$\text{clr}(\pi)(x) = \sum_{\ell=1}^{d+k-1} [\pi]^{C_\ell} Z_\ell(x), \quad (15)$$

where $[\pi]^{C_\ell}$ is the ℓ -th coefficient of π in the CB-spline basis C . Note that the coefficients are the same in the two equations. The coefficients of the global sample mean and regional sample means are readily obtained by

$$\text{clr} \bar{\pi}_g(x) = \frac{1}{n_g} \sum_{i=1}^{n_g} \text{clr} \pi_{gi}(x) \quad (16)$$

$$= \frac{1}{n_g} \sum_{i=1}^{n_g} \sum_{\ell=1}^{d+m-1} [\pi_{gi}]^{C_\ell} \cdot Z_\ell(x) \quad (17)$$

$$= \sum_{\ell=1}^{d+m-1} \left(\frac{1}{n_g} \sum_{i=1}^{n_g} [\pi_{gi}]^{C_\ell} \right) \cdot Z_\ell(x), \quad (18)$$

334 and similarly

$$\text{clr } \bar{\pi}_{..}(x) = \sum_{\ell=1}^{d+m-1} \left(\frac{1}{G} \sum_{g=1}^G \frac{1}{n_g} \sum_{i=1}^{n_g} [\pi_{gi}]^{C_\ell} \right) \cdot Z_\ell(x). \quad (19)$$

335 As in Machalová et al. (2016), after sum-
 336 marizing the initial temperature samples using
 337 histograms, penalized least squares splines are
 338 applied to smooth the data, treating the his-
 339 togram bin centers as the first coordinates and
 340 the corresponding relative frequencies as the sec-
 341 ond coordinates. Figure 2, which displays the
 342 province-level temperature densities grouped by
 343 region, highlights distinct regional patterns in the
 344 temperature distributions.

345 3.3 Temporal trend by province

346 To capture the temporal evolution of tempera-
 347 ture density distributions across provinces within
 348 a given region (or within the whole Vietnam), we
 349 consider a simplified trend model in which each
 350 province’s density evolves linearly over time in
 351 the Bayes space sense. More precisely, if π_{gi}^t now
 352 denotes the density in province i ($i = 1, \dots, n$)
 353 at time t , the simple time evolution model (for
 354 each province) is the following density-on-scalar
 355 regression model:

$$\pi_{gi}^t(x) = [\alpha_{gi} \oplus (t \odot \beta_{gi}) \oplus \varepsilon_{git}](x), \quad (20)$$

356 where β_{gi} is the trend slope density (or simply
 357 slope density) for province i in region g . When
 358 the slope density of this model is the uniform dis-
 359 tribution on (a, b) , there is no observable trend in
 360 the evolution of temperature densities.

361 For estimating the parameters of (20), as in
 362 Talská et al. (2018), the clr transformation is
 363 applied to (20) and the resulting equation is that
 364 of a simple multivariate regression model. The
 365 fitted slopes seem to give a good approximation
 366 of the trend evolution since the coefficients of
 367 determination (defined in the context of density-
 368 on-scalar regression in Talská et al., 2018, p. 79)
 369 range from 63% to 97% (median of 94%) across
 370 provinces, with a better fit in the south. As often
 371 done in functional data, we will treat the resulting
 372 estimators of α_{gi} and β_{gi} as our sample density
 373 dataset (and therefore do not use the hat nota-
 374 tion). In Section 5, we also use the trend density

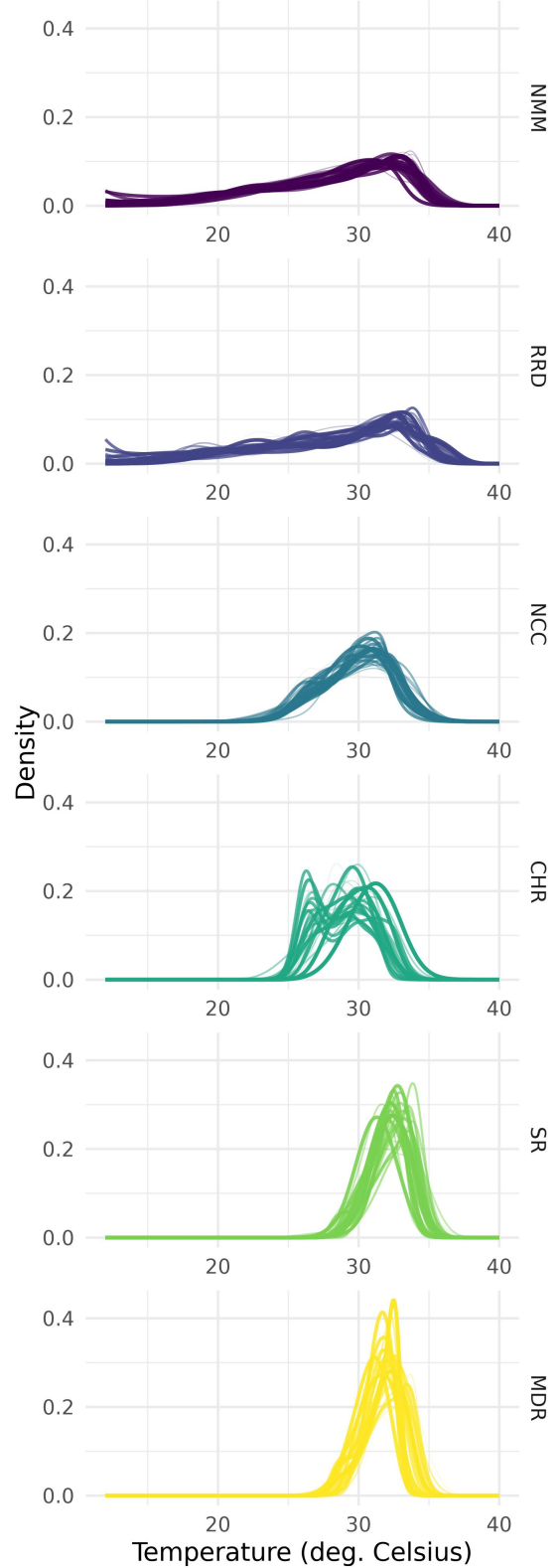


Fig. 2 Regional mean density of maximum temperature across the years 1987 to 2016.

375 functions $\tilde{\pi}_{gi}$ of this model defined by

$$\tilde{\pi}_{gi}^t(x) = [\alpha_{gi} \oplus (t \odot \beta_{gi})](x). \quad (21)$$

376 Figure 3 displays the province specific slope den-
377 sities β_{gi} grouped by region.

378 4 Global tests

379 All testing procedures in this section involve
380 hypotheses about the global behavior of mean
381 densities in the whole interval $[a, b]$. In the appli-
382 cation, the global tests of this section will be
383 applied to the samples of trend slope densities in
384 order to investigate the regional effect on climate
385 change.

386 4.1 One-sample problem

387 In this section, we do not consider a group effect
388 so that $G = 1$ and we temporarily drop the g
389 index resulting in a sample $\pi_i, i = 1, \dots, n$ dis-
390 tributed as π . We are given a reference density
391 π_0 of particular interest and we wish to test the
392 equality to π_0 of the mean density $\mathbb{E}^B(\pi)$:

$$H_0 : \mathbb{E}^B(\pi) = \pi_0. \quad (22)$$

393 Since

$$\begin{aligned} \mathbb{E}^B(\pi) = \pi_0 &\Leftrightarrow \text{clr } \mathbb{E}^B(\pi) = \text{clr } \pi_0 \\ &\Leftrightarrow \mathbb{E}(\text{clr } \pi) = \text{clr } \pi_0, \end{aligned} \quad (23)$$

394 the global one-sample test on mean densities is
395 equivalent to a one sample test in the $L^2(a, b)$
396 space on the clr transformed densities $f_i = \text{clr}(\pi_i)$
397 for which we may apply a classical one sample
398 test for functional data as described in Chap-
399 ter 5 of Zhang (2013). As in Zhang (2013), the
400 functional sample (f_1, \dots, f_n) , is assumed to arise
401 from model (1) (without the regional index g).

402 Two test statistics are available: the L^2 -norm
403 test statistic (Zhang (2013)) and the PC approach
404 (Kokoszka and Reimherr (2017)). We now adapt
405 them to our density framework.

406 L^2 approach. The L^2 -norm statistic yields in the
407 Bayes space

$$T_{\text{norm}} = n \| \text{clr}(\bar{\pi}_{\cdot}) - \text{clr}(\pi_0) \|_{L_0^2(a,b)}^2 \quad (24)$$

408 The asymptotic distribution of this statistic under
409 the null is that of a linear combination of chi-
410 squared statistics weighted by the eigenvalues
411 of the covariance operator, see Kokoszka and
412 Reimherr (2017). For the computation of the

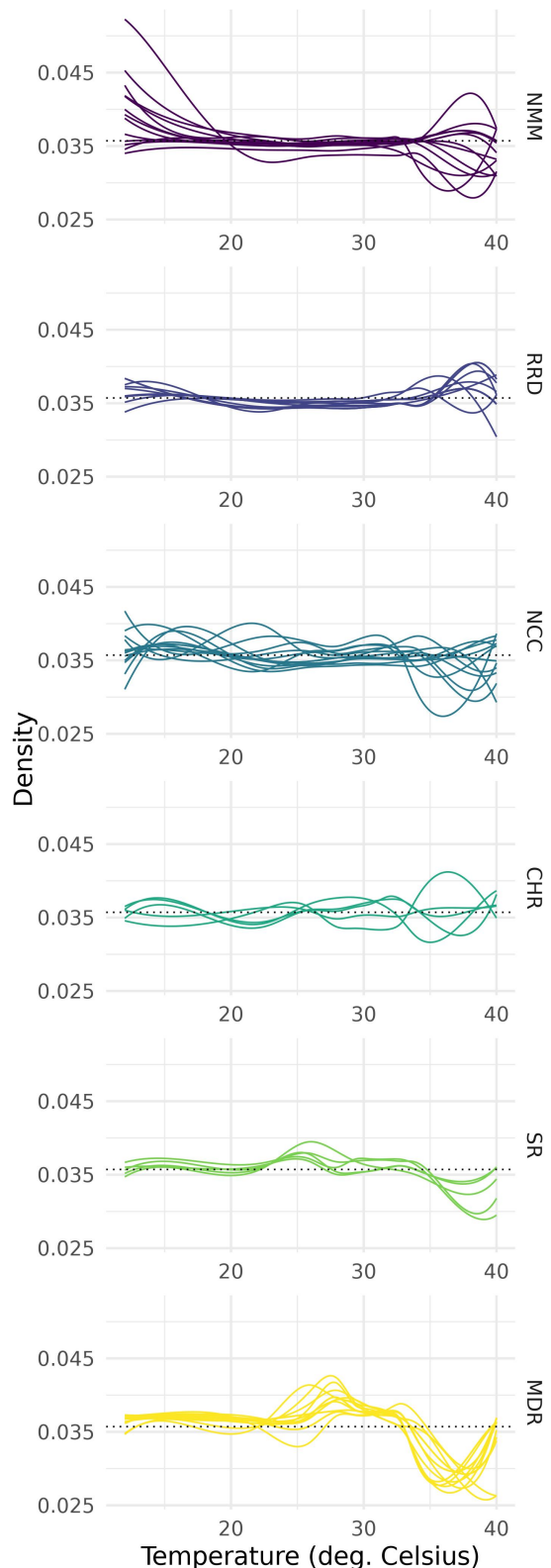


Fig. 3 Trends slopes of provinces grouped by region. The dotted line represents the uniform density on $[12^\circ\text{C}, 40^\circ\text{C}]$ which is the reference measure.

413 p -value of the test, the eigenvalues have to be esti-
 414 mated using FPCA and Kokoszka and Reimherr
 415 (2017) provide code for the computation of the
 416 L^2 -norm.

417 *PC approach.* To eliminate the dependence of
 418 the limiting distribution upon the unknown eigen-
 419 values, Kokoszka and Reimherr (2017) propose
 420 to truncate the Functional Principal Component
 421 Analysis (FPCA) and use a Hotelling-type test
 422 statistic. Keeping the first p terms, the statistic is
 423 given by

$$T_{PC} = n \|\text{clr}(\bar{\pi}_{..}) - \text{clr}(\pi_0)\|_{S^{-1}}^2 \quad (25)$$

$$= n \sum_{k=1}^p \frac{\langle \text{clr}(\bar{\pi}_{..}) - \text{clr}(\pi_0), v_k \rangle_{L_0^2(a,b)}^2}{\hat{\lambda}_k} \quad (26)$$

424 where $\|\cdot\|_{S^{-1}}^2$ is the squared norm weighted by the
 425 inverse of the covariance matrix of the clr coef-
 426 ficients, λ_k are the eigenvalues and v_k the eigen-
 427 functions of the FPCA. Its limiting distribution
 428 under the null is then a simple chi-squared with
 429 p degrees of freedom. Kokoszka and Reimherr
 430 (2017) recommend using the smallest value of p
 431 for which the explained variance exceeds 85%, and
 432 to use the norm approach otherwise.

433 *Application: evolution of temperature* 434 *distributions over the period 1987-2016*

435 Figure 4 displays the global mean trend which
 436 shows that, overall in Vietnam, there is a rela-
 437 tive stability in the central range of tempera-
 438 tures [20°C, 32°C] while low temperatures (below
 439 20°C) tend to become more frequent at the
 440 expense of very high ones above 32°C. The justi-
 441 fication for this statement will be given in Section
 442 5.

443 We perform the one-sample test for the trend
 444 slope sample of β_{gi} . To evaluate the existence
 445 of climate change, we choose π_0 to be the neu-
 446 tral element (uniform density on (a, b)), so that
 447 the null hypothesis represents the absence of cli-
 448 mate change. Both tests in Table 4.1 confirm
 449 the existence of a non-uniform mean trend slope,
 450 indicative of global climate change. We use the fol-
 451 lowing convention for p -values: *** indicate that
 452 the p -value is less than 1% (strong rejection), **
 453 indicate that the p -value is less than 5% (medium
 454 rejection), * indicates that the p -value is less than
 455 10% (weak rejection) and no star means that we
 456 cannot reject the null hypothesis based on the
 457 data.

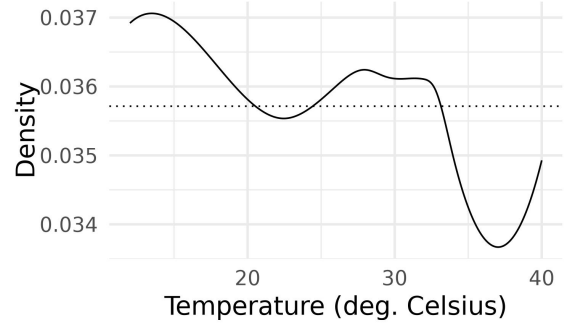


Fig. 4 Global mean trend. The dotted line represents the uniform density on [12°C, 40°C], which is the reference measure.

Name	Statistic	p-value
PC	38	3.1e-08 ***
L^2	1.3	1.3e-06 ***

Table 1 Test statistics and p -values for the global one-sample problem.

458 *Application: regional evolution of* 459 *temperature distributions over the period* 460 *1987-2016*

461 After testing the existence of global climate
 462 change, it may be interesting to perform a one-
 463 sample test in each region separately to see
 464 whether climate change does not affect some
 465 regions. The corresponding Šidák-adjusted p -
 466 values (see Abdi, 2010) are displayed in Table
 467 2. This table strongly supports the existence of
 468 climate change in the Red River Delta (RRD)
 469 region and in the southern regions SR and MDR,
 470 the non-existence of climate change in the Cen-
 471 tral Highlands (CHR) region. The results are
 472 more contrasted in the Northern Midlands and
 473 Mountains (NMM) region and in the North Cen-
 474 tral Coast (NCC) region where the tests are
 475 either non-significant or very marginally signifi-
 476 cant. These results should be interpreted with
 477 caution due to the small sample size in each
 478 region.

Region	Sample size	PC	L^2
NMM	14	7.9e-02 *	0.12
RRD	12	1.6e-10 ***	1.5e-04 ***
NCC	13	8e-02 *	0.12
CHR	5	0.65	0.99
SR	6	1.8e-03 ***	4.2e-04 ***
MDR	13	0 ***	4.9e-08 ***

Table 2 Šidák-adjusted p -values for the regional one sample test.

4.2 Distributional ANOVA

Using the notations of Section 2, the objective of DANOVA is to test the null hypothesis H_0 that the G group mean densities $\mathbb{E}^B(\pi_g)$ are equal against the usual alternative that at least two means are different, where mean density here is understood in the Bayes space sense:

$$H_0 : \forall g, \quad \mathbb{E}^B(\pi_{gi}) = \mathbb{E}^B(\pi_{1i}). \quad (27)$$

Let us first note that for two densities π_1 and π_2 we have the following equivalence

$$\mathbb{E}^B(\pi_1) = \mathbb{E}^B(\pi_2) \Leftrightarrow \mathbb{E}(\text{clr } \pi_1) = \mathbb{E}(\text{clr } \pi_2), \quad (28)$$

since the clr of the expected density in the Bayes sense is equal to the expected value in the classical sense of the clr of the density in the corresponding L_0^2 space. Therefore, the assumption (27) is equivalent to

$$H_0 : \forall g, \quad \mathbb{E}(\text{clr } \pi_{gi}) = \mathbb{E}(\text{clr } \pi_{1i}). \quad (29)$$

In order to adapt FANOVA to DANOVA, we can thus simply apply the FANOVA techniques to the clr transformed densities in the functional space L_0^2 . The R package `fdANOVA` (described in [Górecki and Smaga, 2019](#)) provides several FANOVA options and we focus on the following five test statistics. Their evaluation requires the computation of the following quantities: the pointwise variations $\text{SSB}(x)$ and $\text{SSW}(x)$ from (12) and (13), and pairwise negative perturbations between group means for the statistic proposed by [Cuevas et al. \(2004\)](#). The coefficients of the required clr transforms in a chosen ZB-basis are easily computed from the coefficients of the clr of $\pi_{gi}, \bar{\pi}_g, \bar{\pi}_{..}$, the last two being obtained by (16) and (19). Let us briefly describe the five test statistics and try to provide when possible a Bayes space expression.

1. The L^2 -norm based test statistic from [Zhang and Chen \(2007\)](#) is given in the framework of ANOVA by

$$L^2B = \int_a^b \text{SSB}(x) dx, \quad (30)$$

where $\text{SSB}(x)$ is given by (4). Note that an alternative formula for L^2B when applied to clr of densities is directly given in the Bayes space by

$$L^2B = \sum_{g=1}^G n_g \|\bar{\pi}_g \ominus \bar{\pi}_{..}\|_{B^2}^2, \quad (31)$$

which shows that this statistic can be expressed as a norm and is therefore invariant under almost-everywhere equality. In the [Górecki and Smaga \(2019\)](#) R package, the `L2B` implementation uses an asymptotic distribution of the test statistic.

2. The F-type tests from [Shen and Faraway \(2004\)](#) and [Zhang \(2011\)](#) use both within and between variation:

$$\begin{aligned} \text{FB} &= \frac{\int_a^b \text{SSB}(x) dx / (G-1)}{\int_a^b \text{SSW}(x) dx / (n-G)} \\ &= \frac{\sum_{g=1}^G n_g \|\bar{\pi}_g \ominus \bar{\pi}_{..}\|_{B^2}^2 / (G-1)}{\sum_{g=1}^G \sum_{i=1}^{n_g} \|\pi_{gi} \ominus \bar{\pi}_g\|_{B^2}^2 / (n-G)}. \end{aligned} \quad (32)$$

We choose the FB implementation (biased-reduced) for the computation of the p -value. Under the null hypothesis, this statistic is asymptotically equal to a linear combination of independent χ^2 for the numerator and the denominator, and can thus be approximated by a Fischer distribution ([Zhang, 2011](#), Theorem 1 and equation (2.16)). The test statistic coincides with that of [Van Den Boogaart et al. \(2014\)](#) by the second equality in (32). However, [Van Den Boogaart et al. \(2014\)](#) use a bootstrap procedure rather than the above approximation.

3. The CS statistic from [Cuevas et al. \(2004\)](#) uses pairwise differences. When applied to clr of densities, due to the linearity of clr, we get

$$\begin{aligned} \text{CS} &= \sum_{g < g'} n_g \int_a^b (\text{clr } \bar{\pi}_g(x) - \text{clr } \bar{\pi}_{g'}(x))^2 dx \\ &= \sum_{g < g'} n_g \|\bar{\pi}_g \ominus \bar{\pi}_{g'}\|_{B^2}^2 \end{aligned} \quad (33)$$

The CS implementation in the `fdANOVA` package uses a heteroscedastic assumption and parametric bootstrap. Note that an alternative formula for CS is the sum of the Bayes norms of all pairwise differences between groups.

4. The GPF statistic from [Zhang and Liang \(2014\)](#) integrates the pointwise F-ratio instead of integrating separately the pointwise within and between variations:

$$\text{GPF} = \int_a^b \frac{\text{SSB}(x)/(G-1)}{\text{SSW}(x)/(n-G)} dx. \quad (34)$$

Under the null hypothesis, this statistic is asymptotically equal to a linear combination

553 of independent χ^2 , which can be approximated
 554 by a χ^2 -distribution (Zhang and Liang, 2014,
 555 Proposition 1). In the implementation of the
 556 fdANOVA package, GPF is divided by $b - a$, and
 557 the null distribution is modified accordingly.
 558 Górecki and Smaga (2018) (page 5) claim that
 559 the GPF test is more powerful than the F-type
 560 tests.

561 5. The F_{\max} statistic from Zhang et al. (2019)
 562 rather computes the supremum of the point-
 563 wise F-ratio instead of integrating it as in
 564 GPF:

$$F_{\max} = \sup_{x \in (a,b)} \frac{SSB(x)/(G-1)}{SSW(x)/(n-G)}. \quad (35)$$

565 We consider the implementation $F_{\max b}$ which
 566 bootstraps the distribution under the null
 567 hypothesis. The statistic F_{\max} is the only one
 568 that is not invariant under almost-everywhere
 569 equality: changing one value of a density in the
 570 dataset might change the value of F_{\max} . Note
 571 also that the statistics GPF and F_{\max} cannot
 572 be written straightforwardly in terms of norms
 573 in the Bayes space.

574 **Application: regional evolution of**
 575 **temperature distribution over the period**
 576 **1987-2016**

577 Figure 5 displays the regional mean trend slope
 578 densities. For the central regions (CHR and
 579 NCC), this plot shows a relative stability of the
 580 maximum temperature distribution (the trend is
 581 not far from uniform). For the RRD region, the
 582 curve exhibits a noticeable bump above the uni-
 583 form on the right tail. More details about the
 584 interpretation of these curves will be given in
 585 Section 5.

586 We now test whether these trend densities
 587 vary across regions. Table 3 summarizes the
 588 results of the global analysis of variance for which
 589 the above tests all conclude that there is a differ-
 590 ence in the way the regional temperature densities
 591 evolve in time.

Name	Statistic	p -value
GPF	10	0 ***
Fmaxb	36	0 ***
CS	700	0 ***
L2B	130	0 ***
FB	9.9	0 ***

Table 3 Test statistics and p -values for DANOVA.

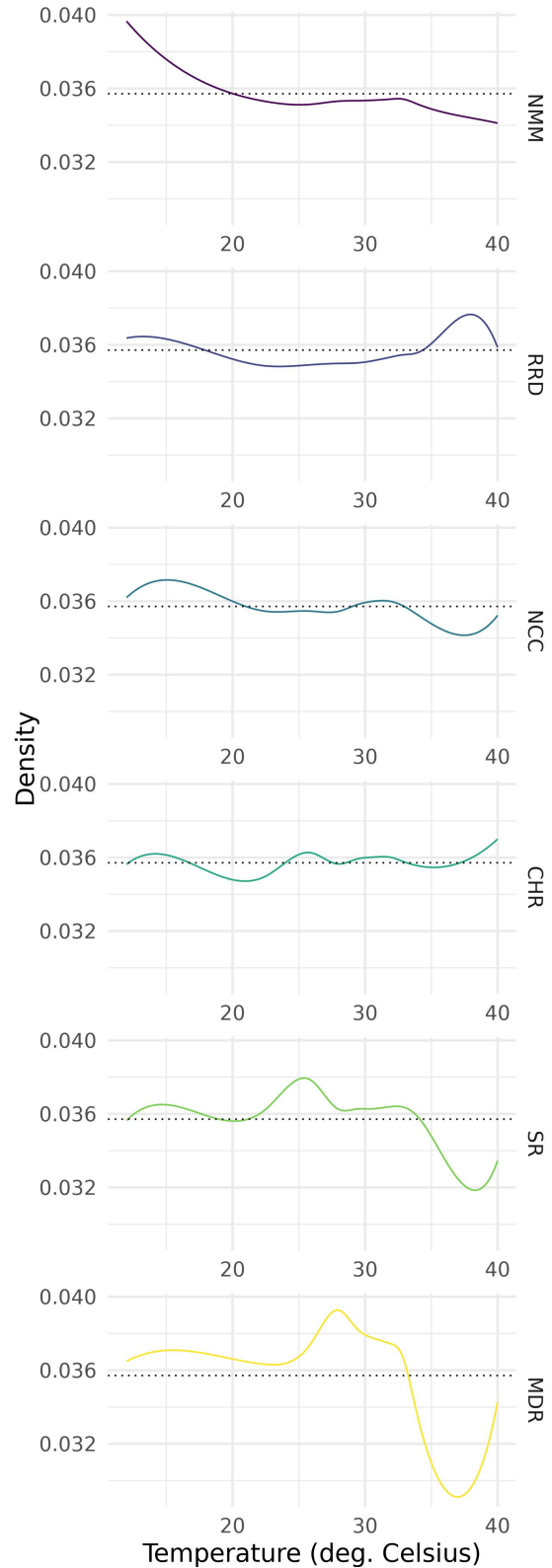


Fig. 5 Regional mean trend slopes. The dotted line represents the uniform density on $[12^\circ\text{C}, 40^\circ\text{C}]$ which is the reference measure.

4.3 Pairwise comparisons

When the test of equality of group mean densities is significant, conducting a post-hoc analysis of pairwise group mean comparisons can help identify which pairs differ. The null hypothesis for comparing groups g and g' is:

$$H_0 : \mathbb{E}^B(\pi_{gi}) = \mathbb{E}^B(\pi_{g'i}),$$

which is equivalent to

$$H_0 : \mathbb{E}(\text{clr } \pi_{gi}) = \mathbb{E}(\text{clr } \pi_{g'i}).$$

Testing whether the mean density in group g_1 is equal to the mean density in group g_2 can be viewed as a two-sample ANOVA test. A multiple testing correction is necessary when performing these tests for all pairs of groups.

Application: regional evolution of temperature distribution over the period 1987-2016

Table 4 displays the tests statistics with their Šidák-adjusted p -values for the five pairwise tests. We summarize and visualize these results on Figure 6 by drawing

1. a solid line between two regions when the equality of mean slope densities is rejected by all five tests
2. a dotted line between two regions when the equality of mean slope densities is rejected by some but not all of the five tests
3. no line between two regions when the equality of mean slope densities is rejected by all five tests.

The small number of dotted lines supports the fact that the five tests agree most of the time. The structure of Figure 6 is interestingly similar to the geographical structure of the regions (see the map on Figure 1) with solid lines between neighbouring regions. It shows that the Mekong Delta region differs statistically from most other regions in terms of climate change. Among the remaining regions, the Red River Delta region differs the most from the others in the sense that it is only connected by dotted lines.

5 Interval-wise interpretation

The global tests presented in the previous section, whether one-sample tests or analysis of variance, enable us to draw inferences about differences in the behavior of mean densities across the entire temperature range. Now, we aim to make more localized statements regarding regional differences in temporal evolution, particularly within specific temperature intervals.

Region 1	Region 2	L2B	FB	CS
NMM	RRD	1e-01 *	0.18	0 ***
NMM	NCC	1	1	1
NMM	CHR	0.97	0.99	0.96
NMM	SR	0.71	0.83	0.26
NMM	MDR	5.4e-09 ***	1.4e-06 ***	0 ***
RRD	NCC	2.5e-03 ***	8.6e-03 ***	0 ***
RRD	CHR	0.82	0.89	1
RRD	SR	8.7e-11 ***	3.9e-06 ***	0 ***
RRD	MDR	0 ***	0 ***	0 ***
NCC	CHR	0.99	1	0.99
NCC	SR	0.6	0.71	0.14
NCC	MDR	7.9e-13 ***	2.6e-09 ***	0 ***
CHR	SR	0.15	0.4	0.46
CHR	MDR	3.7e-11 ***	2.3e-07 ***	0 ***
SR	MDR	9e-04 ***	6.2e-03 ***	0 ***

Region 1	Region 2	GPF	Fmaxb
NMM	RRD	0.33	0.85
NMM	NCC	1	0.97
NMM	CHR	0.48	0.37
NMM	SR	3e-05 ***	0 ***
NMM	MDR	0 ***	0 ***
RRD	NCC	2.8e-02 **	0 ***
RRD	CHR	3.3e-02 **	0 ***
RRD	SR	0 ***	0 ***
RRD	MDR	0 ***	0 ***
NCC	CHR	0.98	0.96
NCC	SR	0.49	0.14
NCC	MDR	2e-13 ***	0 ***
CHR	SR	0.27	0.54
CHR	MDR	4.8e-11 ***	0 ***
SR	MDR	2.7e-06 ***	0.14

Table 4 Šidák-adjusted p -values for pairwise group mean comparison.

Unfortunately, the idea of adapting local tests from FANOVA does not work for two reasons. First of all, the meaning of a test of the equality of two mean densities evaluated at a given point x is unclear since densities are only defined almost everywhere, unless we impose continuity restrictions. The second reason is that the equivalence (28) between the equality of two mean densities and the equality of their clr transform is not valid anymore at the local level because the clr transform evaluated at x involves all values of the log density and not only its value at x .

For these reasons, we turn attention to some interpretation tools presented in Maier et al. (2024) based on odds ratios.

5.1 Infinitesimal odds ratios

We focus on subintervals $I \subset (a, b)$ and wish to assess the time evolution of the relative probability to be in one interval versus the other.

We can rely on (Maier et al., 2024, pp. 10 and 11, Proposition 3.1) for the definition of the infinitesimal odds ratios and their interpretation. The objective is to compare the value of a slope

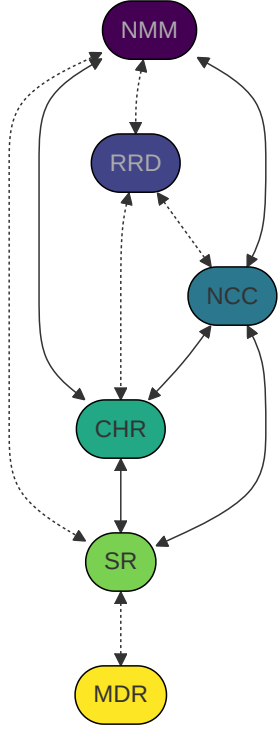


Fig. 6 Summary of pairwise tests between regions of Vietnam. Solid line: no test rejects the null hypothesis; dotted line: some tests reject the null hypothesis; absence of line: all tests reject the null hypothesis.

density β_{gi} and β_g . (we call it β in this paragraph) at two different temperature values x and z in the temperature range. Let us define the relative frequency $OR_{x|z}(\beta)$ of a density β at two points x and z by

$$OR_{x|z}(\beta) = \frac{\beta(x)}{\beta(z)} \quad (36)$$

For $\beta = \beta_{gi}$ in model (20), let us show that this quantity is indeed an infinitesimal odds ratio relative to the trend densities $\tilde{\pi}_{it}(z)$. Indeed, by linearity of model (20), we have that for all t ,

$$\frac{\beta_{gi}(x)}{\beta_{gi}(z)} = \frac{\tilde{\pi}_{gi}^{t+1}(x) \ominus \tilde{\pi}_{gi}^t(x)}{\tilde{\pi}_{gi}^{t+1}(z) \ominus \tilde{\pi}_{gi}^t(z)}$$

and therefore

$$OR_{x|z}(\beta_{gi}) = \frac{\frac{\tilde{\pi}_{gi}^{t+1}(x)}{\tilde{\pi}_{gi}^{t+1}(z)}}{\frac{\tilde{\pi}_{gi}^t(x)}{\tilde{\pi}_{gi}^t(z)}} \quad (37)$$

is the ratio of the odds of x versus z at time $t+1$ by the odds of x versus z at time t . We thus see that the relative change of the odds of x versus z in the period $(t, t+1)$ is equal to $\frac{\beta(x)}{\beta(z)} - 1$. Note that

this relative change formula is only valid within our simple linear trend model.

According to part (a) of Proposition 3.1 in Maier et al. (2024), if we observe that $OR_{x|z}(\beta_{gi}) > 1$ for all x, z when x is in a given interval A and z in a given interval B for a given slope density β_{gi} , then we may conclude that conditional on the temperature being in A or B , the odds (according to the density $\tilde{\pi}_{gi}^{t+1}$) of being in A at time $t+1$ are larger than the odds (according to the trend density $\tilde{\pi}_{gi}^t$) of being in A at time t . Because the probability of an event is an increasing function of its odds, same is true for the corresponding probabilities so that there has been a mass transfer of the probability mass of the trend density from B to A between t and $t+1$.

Using the fact that $OR_{x|z}(\beta_{gi}) > 1$ is equivalent to $\beta_{gi}(x) > \beta_{gi}(z)$, we are going to show that the curve of β_{gi} allows to draw conclusions about the temperature density changes as follows. For a given level $\tau = \beta_{gi}(x_0) > 0$, let the collection of intervals (or unions of intervals) $A_\tau(\beta_{gi})$ be defined by $A_\tau(\beta_{gi}) = \{x : \beta_{gi}(x) > \tau\}$. Let $A_\tau^c(\beta_{gi})$ be the complement of $A_\tau(\beta_{gi})$. Then we have for almost all $x \in A_\tau(\beta_{gi})$ and almost all $z \in A_\tau^c(\beta_{gi})$

$$OR_{x|z}(\beta_{gi}) = \frac{\beta(x)}{\beta(x_0)} \frac{\beta(x_0)}{\beta(z)} > 1, \quad (38)$$

Therefore, we may say that the probability that it lies in $A_\tau(\beta_{gi})$ according to the trend density at time $t+1$ (i.e. under the distribution $\tilde{\pi}^{t+1}$) is higher than that according to the trend density at time t (i.e. under the distribution $\tilde{\pi}^t$). We will consider various values of the level τ increasing from the minimum to the maximum of the slope density and comment the corresponding interpretations.

5.2 Global change in temperature distribution over the period 1987-2016

Next we apply these interpretations to the global slope density $\beta_{..}$. From (37) we can derive that

$$OR_{x|z}(\beta_{..}) = \frac{\frac{\tilde{\pi}_{..}^{t+1}(x) \ominus \tilde{\pi}_{..}^t(x)}{\tilde{\pi}_{..}^{t+1}(z) \ominus \tilde{\pi}_{..}^t(z)}}{\frac{\tilde{\pi}_{..}^t(x)}{\tilde{\pi}_{..}^t(z)}} \quad (39)$$

On Figure 7, using a first level of 0.0362 represented by a horizontal line, we see that on average in Vietnam low temperatures below 18.2°C become relatively more frequent than temperatures above 18.2°C. Similarly, with a second level of 0.0355, we see that on average in Vietnam high

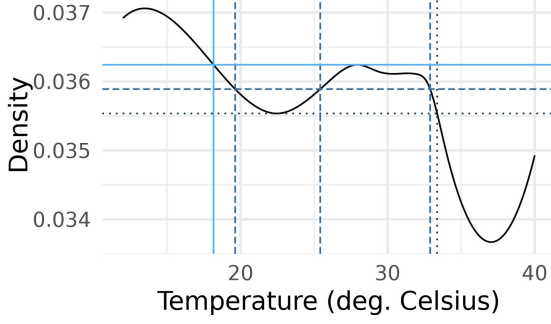


Fig. 7 Global mean slope density with three levels.

724 temperatures above 33.4°C become relatively
 725 more frequent than temperatures below 33.4°C.
 726 However these two statements need to be put into
 727 perspective due to the scarcity of observations at
 728 the extremes. More importantly, focusing now on
 729 the range [19.6°C, 32.9°C] and the level 0.0359,
 730 we can say that the frequency of temperatures
 731 within the interval [19.6°C, 25.4°C] has decreased
 732 over time relative to those in [25.4°C, 32.9°C],
 733 supporting a global warming trend. Technically,
 734 this assertion corresponds to the interpretation of
 735 a conditional probability statement.

736 5.3 Regional changes in 737 temperature distribution over 738 the period 1987-2016

739 Similarly, when comparing the regional slope den-
 740 sity β_g , at two temperature points x and z , we use
 741 $OR_{x|z}(\beta_g)$. From (37) we can derive that

$$OR_{x|z}(\beta_g) = \frac{\tilde{\pi}_g^{t+1}(x) \ominus \tilde{\pi}_g^t(x)}{\tilde{\pi}_g^{t+1}(z) \ominus \tilde{\pi}_g^t(z)} = \frac{\frac{\tilde{\pi}_g^{t+1}(x)}{\tilde{\pi}_g^{t+1}(z)}}{\frac{\tilde{\pi}_g^t(x)}{\tilde{\pi}_g^t(z)}} \quad (40)$$

742 Figures 8, 9 and 10 display the slope densities
 743 of the six regions with some chosen values of level
 744 τ . We are able to group the regions in terms of
 745 the shape of their mean slope density.

746 Based on Figure 8, in mountainous regions,
 747 as for the global trend, the small and high val-
 748 ues of τ demonstrate an increase of the frequency
 749 of low temperatures. Provided we focus on the
 750 medium range ([22.6°C, 27.6°C] for NMM and
 751 [21°C, 29.1°C] for NCC), the intermediate values
 752 of τ show a shift towards higher temperatures.

753 Based on Figure 9, the RRD and CHR regions
 754 display an increasing spread of their tempera-
 755 ture distribution over time (small values of τ)
 756 and an increase of extremely high temperature

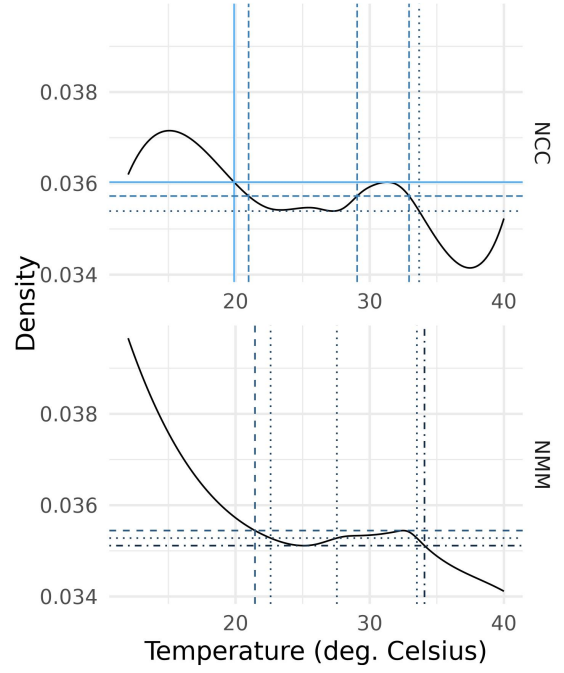


Fig. 8 Mean slope densities of North Central Coast (NCC) and Northern Midlands and Mountains (NMM) regions with levels.

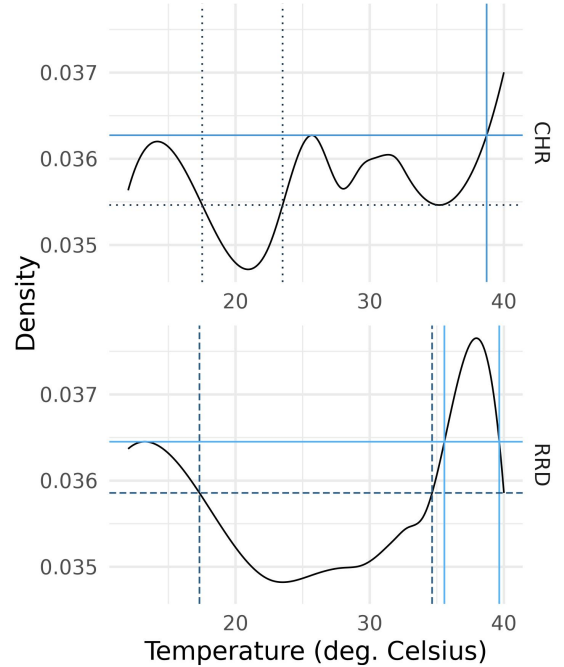


Fig. 9 Mean slope densities of Red River Delta (RRD) and Central Highlands (CHR) regions with levels.

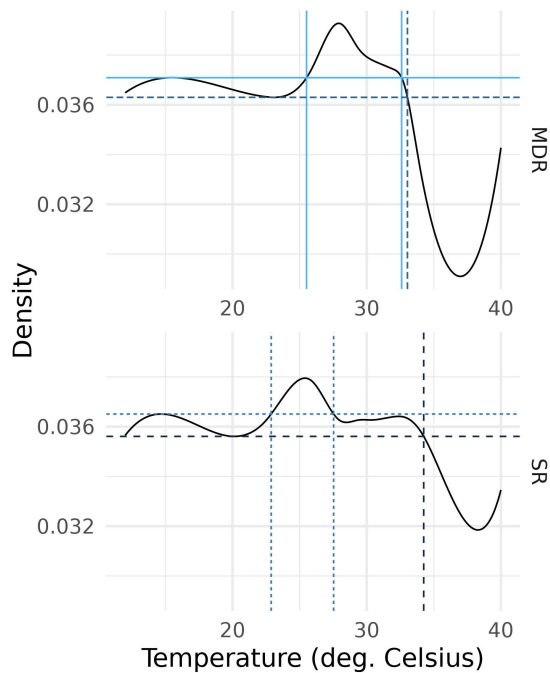


Fig. 10 Mean slope densities of Southeast (SR) and Mekong Delta (MDR) regions with levels.

757 events (high values of τ). Note that since temper-
 758 ature change is not detected in the CHR region
 759 (Table 3), its interpretation based on odds ratio
 760 is probably not reliable.

761 Based on Figure 10, the south in contrast
 762 shows a concentration in the medium range
 763 around 25°C for SR and 28°C for MDR at the
 764 expense of high temperatures.

765 While these groups reflect the geography (lati-
 766 tude and elevation) of Vietnam, they are also con-
 767 sistent with the groups suggested by the regional
 768 one-sample tests (Table 2) and the pairwise com-
 769 parisons (Table 4).

770 6 Conclusion

771 We have adapted several functional data analy-
 772 sis tests to density functions in order to assess
 773 the equality of mean densities and to perform
 774 DANOVA tests in the framework of Bayes spaces.
 775 In our target application of temperature density
 776 evolution in Vietnam, the one-sample test allows
 777 to conclude that there is statistical evidence of a
 778 climate change in Vietnam in the sense that the
 779 trend slope density is not uniform. Furthermore,
 780 when considering the functions globally, most of
 781 the DANOVA statistics strongly reject the null
 782 hypothesis, that is, the equality of trend slope
 783 density across the Vietnamese regions. For more

784 local interpretations, we rely on the infinitesi-
 785 mal odds ratio of Maier et al. (2025). These
 786 local investigations remain exploratory, and ele-
 787 vating them to formal tests presents an interesting
 788 avenue for future research. Needless to say that
 789 the proposed methodology can be applied in other
 790 application frameworks. Future research might
 791 try to reduce the uncertainty due to the low den-
 792 sity of extreme temperatures, possibly weighting
 793 the domain of the Bayes space as in Talská et al.
 794 (2020). This methodology is promising for envi-
 795 ronmental studies, with a possible application for
 796 example to the relative concentrations of contam-
 797 inants in grounds or rivers analyzed as density
 798 functions.

799 Acknowledgments

800 Part of this work was completed while the authors
 801 were visiting the Vietnam Institute for Advanced
 802 Study in Mathematics (VIASM) in Hanoi and
 803 the authors express their gratitude to VIASM.
 804 We also acknowledge funding from the French
 805 National Research Agency (ANR) under grant
 806 ANR-17-EURE-0010 (Investissements d’Avenir
 807 program), from the French National Associa-
 808 tion of Research and Technology (ANRT), grant
 809 CIFRE n°2020/0011, and from Spanish Min-
 810 isterio de Ciencia e Innovación grant number
 811 PID2021-123833OB-I00.

812 Code & reproducibility

813 In order to implement DANOVA, we created the
 814 R package ICSFun, available at:

815 <https://github.com/camillemndn/dda>

816 This article and its figures are fully reproducible
 817 using the code available at:

818 <https://github.com/camillemndn/danova>

819 References

- 820 Abdi, H.: Holm’s Sequential Bonferroni Proce-
 821 dure. In: Encyclopedia of Research Design, pp.
 822 574–577. SAGE Publications, Inc., ??? (2010).
 823 <https://doi.org/10.4135/9781412961288>
 824 <https://methods.sagepub.com/ency/edvol/encyc->
 825 [of-research-design/chpt/holms-sequential-](https://methods.sagepub.com/ency/edvol/encyc-)
 826 [bonferroni-procedure](https://methods.sagepub.com/ency/edvol/encyc-) Accessed 2025-06-24
- 827 Aneiros, G., Horová, I., Hušková, M., Vieu,
 828 P.: On functional data analysis and related
 829 topics. *Journal of Multivariate Analysis* **189**,
 830 104861 (2022) [https://doi.org/10.1016/j.jmva.](https://doi.org/10.1016/j.jmva.2021.104861)
 831 [2021.104861](https://doi.org/10.1016/j.jmva.2021.104861)

- 832 Cuevas, A., Febrero, M., Fraiman, R.: An anova 881
833 test for functional data. *Computational Statistics & Data Analysis* **47**(1), 111–122 (2004) 882
834 <https://doi.org/10.1016/j.csda.2003.10.021> 883
835 884
- 836 Espagne, E., Diallo, Y., Marchand, S.: Impacts 885
837 of Extreme Climate Events on Technical 886
838 Efficiency in Vietnamese Agriculture. Number: 887
839 c1221ee7-5311-4af0-b1b4-3972fc637a9f 888
840 Publisher: Agence française de développement 889
841 (2019). [https://ideas.repec.org/p/avg/](https://ideas.repec.org/p/avg/wpaper/en9476.html) 890
842 [wpaper/en9476.html](https://ideas.repec.org/p/avg/wpaper/en9476.html) Accessed 2024-05-20 891
- 843 Egozcue, J.J., Díaz-Barrero, J.L., 892
844 Pawlowsky-Glahn, V.: Hilbert Space of 893
845 Probability Density Functions Based on 894
846 Aitchison Geometry. *Acta Mathematica Sinica, English Series* **22**(4), 1175–1182 (2006) 895
847 <https://doi.org/10.1007/s10114-005-0678-2> 896
848 897
- 849 Gubler, S., Fukutome, S., Scherrer, S.C.: On 898
850 the statistical distribution of temperature and 899
851 the classification of extreme events considering 900
852 season and climate change—an application in 901
853 Switzerland. *Theoretical and Applied Climatology* **153**(3-4), 1273–1291 (2023) [https://doi.](https://doi.org/10.1007/s00704-023-04530-0) 902
854 [org/10.1007/s00704-023-04530-0](https://doi.org/10.1007/s00704-023-04530-0) 903
855 904
- 856 Górecki, T., Smaga, L.: fdANOVA: Analysis of 905
857 Variance for Univariate and Multivariate Func- 906
858 tional Data (2018). [https://cran.r-project.org/](https://cran.r-project.org/web/packages/fdANOVA/index.html) 907
859 [web/packages/fdANOVA/index.html](https://cran.r-project.org/web/packages/fdANOVA/index.html) Accessed 908
860 2024-03-14 909
- 861 Górecki, T., Smaga, L.: fdANOVA: an R software 910
862 package for analysis of variance for univariate 911
863 and multivariate functional data. *Computational Statistics* **34**(2), 571–597 (2019) [https:](https://doi.org/10.1007/s00180-018-0842-7) 912
864 [//doi.org/10.1007/s00180-018-0842-7](https://doi.org/10.1007/s00180-018-0842-7) 913
865 914
- 866 Hultgren, A., Carleton, T., Delgado, M., Gergel, 915
867 D.R., Greenstone, M., Houser, T., Hsiang, 916
868 S., Jina, A., Kopp, R.E., Malevich, S.B., 917
869 McCusker, K., Mayer, T., Nath, I., Rising, J., 918
870 Rode, A., Yuan, J.: Estimating Global Impacts 919
871 to Agriculture from Climate Change Account- 920
872 ing for Adaptation. *SSRN Electronic Journal* 921
873 (2022) <https://doi.org/10.2139/ssrn.4222020> 922
- 874 Hsiang, S., Kopp, R., Jina, A., Rising, J., Delgado, 923
875 M., Mohan, S., Rasmussen, D.J., Muir-Wood, 924
876 R., Wilson, P., Oppenheimer, M., Larsen, K., 925
877 Houser, T.: Estimating economic damage from 926
878 climate change in the United States. *Science* 927
879 **356**(6345), 1362–1369 (2017) [https://doi.org/](https://doi.org/10.1126/science.aal4369) 928
880 [10.1126/science.aal4369](https://doi.org/10.1126/science.aal4369) 929
- Kokoszka, P., Reimherr, M.: Introduction to 881
Functional Data Analysis, 1st edn. Chapman 882
and Hall/CRC, ??? (2017). [https://doi.org/10.](https://doi.org/10.1201/9781315117416) 883
[1201/9781315117416](https://doi.org/10.1201/9781315117416) 884
- Martín-Fernández, J.-A., Daunis-i-Estadella, J., 885
Mateu-Figueras, G.: On the interpretation 886
of differences between groups for composi- 887
tional data. *SORT-Statistics and Operations* 888
Research Transactions **39**(2), 231–252 (2015). 889
Number: 2. Accessed 2024-03-11 890
- Machalová, J., Hron, K., Monti, G.S.: Prepro- 891
cessing of centred logratio transformed den- 892
sity functions using smoothing splines. *Journal of Applied Statistics* **43**(8), 1419–1435 893
(2016) [https://doi.org/10.1080/02664763.2015.](https://doi.org/10.1080/02664763.2015.1103706) 894
[1103706](https://doi.org/10.1080/02664763.2015.1103706) 895
- Maier, E.-M., Stöcker, A., Fitzenberger, B., 897
Greven, S.: Additive Density-on-Scalar Regres- 898
sion in Bayes Hilbert Spaces with an 899
Application to Gender Economics. *arXiv.* 900
arXiv:2110.11771 [stat] (2024). [https://doi.](https://doi.org/10.48550/arXiv.2110.11771) 901
[org/10.48550/arXiv.2110.11771](https://doi.org/10.48550/arXiv.2110.11771) . [http://arxiv.](http://arxiv.org/abs/2110.11771) 902
[org/abs/2110.11771](http://arxiv.org/abs/2110.11771) Accessed 2025-02-25 903
- Maier, E.-M., Stöcker, A., Fitzenberger, B., 904
Greven, S.: Additive density-on-scalar regres- 905
sion in Bayes Hilbert spaces with an applica- 906
tion to gender economics. *The Annals of* 907
Applied Statistics **19**(1), 680–700 (2025) [https:](https://doi.org/10.1214/24-AOAS1979) 908
[//doi.org/10.1214/24-AOAS1979](https://doi.org/10.1214/24-AOAS1979) . Publisher: 909
Institute of Mathematical Statistics. Accessed 910
2025-03-18 911
- Machalová, J., Talská, R., Hron, K., Gába, 912
A.: Compositional splines for representation 913
of density functions. *Computational Statistics* 914
36(2), 1031–1064 (2021) [https://doi.org/10.](https://doi.org/10.1007/s00180-020-01042-7) 915
[1007/s00180-020-01042-7](https://doi.org/10.1007/s00180-020-01042-7) 916
- Petersen, A., Zhang, C., Kokoszka, P.: Modeling 917
Probability Density Functions as Data Objects. 918
Econometrics and Statistics **21**, 159–178 (2022) 919
<https://doi.org/10.1016/j.ecosta.2021.04.004> 920
- Ramsay, J.O., Silverman, B.W.: *Functional Data* 921
Analysis. Springer Series in Statistics. Springer, 922
New York, NY (2005). [https://doi.org/10.](https://doi.org/10.1007/b98888) 923
[1007/b98888](https://doi.org/10.1007/b98888) 924
- Roberts, M.J., Schlenker, W., Eyer, J.: Agro- 925
nomic Weather Measures in Econometric Mod- 926
els of Crop Yield with Implications for Climate 927
Change. *American Journal of Agricultural Eco-* 928
nomics **95**(2), 236–243 (2013) <https://doi.org/> 929

- 10.1093/ajae/aas047
- Schumaker, L.: Spline Functions: Basic Theory, 3rd edn. Cambridge University Press, ??? (1981). <https://doi.org/10.1017/CBO9780511618994>
- Shen, Q., Faraway, J.: An F Test for Linear Models with Functional Responses. *Statistica Sinica* **14**(4), 1239–1257 (2004). Publisher: Institute of Statistical Science, Academia Sinica. Accessed 2025-02-11
- Schlenker, W., Roberts, M.J.: Nonlinear temperature effects indicate severe damages to U.S. crop yields under climate change. *Proceedings of the National Academy of Sciences* **106**(37), 15594–15598 (2009) <https://doi.org/10.1073/pnas.0906865106>
- Trinh, T.-A., Feeny, S., Posso, A.: The Impact of Natural Disasters and Climate Change on Agriculture: Findings From Vietnam. In: *Economic Effects of Natural Disasters*, pp. 261–280. Elsevier, ??? (2021). <https://doi.org/10.1016/B978-0-12-817465-4.00017-0>
- Talská, R., Menafoglio, A., Hron, K., Egozcue, J.J., Palarea-Albaladejo, J.: Weighting the domain of probability densities in functional data analysis. *Stat* **9**(1), 283 (2020) <https://doi.org/10.1002/sta4.283> . Accessed 2024-01-06
- Talská, R., Menafoglio, A., Machalová, J., Hron, K., Fišerová, E.: Compositional regression with functional response. *Computational Statistics & Data Analysis* **123**, 66–85 (2018) <https://doi.org/10.1016/j.csda.2018.01.018> . Accessed 2025-03-05
- Tran, T.D., Nguyen, T.V.: Climate Change Adaptation in Vietnam." In *Climate Change Adaptation in Southeast Asia*. Singapore: Springer Singapore, ??? (2021)
- Trinh, T.A.: The Impact of Climate Change on Agriculture: Findings from Households in Vietnam. *Environmental and Resource Economics* **71**(4), 897–921 (2018) <https://doi.org/10.1007/s10640-017-0189-5>
- Trinh, H.T., Thomas-Agnan, C., Simioni, M.: Discrete and Smooth Scalar-on-Density Compositional Regression for Assessing the Impact of Climate Change on Rice Yield in Vietnam. TSE Working Paper **23-1410** (2023)
- Van Den Boogaart, K.G., Egozcue, J.J., Pawlowsky-Glahn, V.: Bayes linear spaces. *SORT : statistics and operations research transactions* **34**, 201–222 (2010)
- Van Den Boogaart, K.G., Egozcue, J.J., Pawlowsky-Glahn, V.: Bayes Hilbert spaces. *Australian & New Zealand Journal of Statistics* **56**(2), 171–194 (2014) <https://doi.org/10.1111/anzs.12074>
- Vo, T.H., Nguyen, V.T., Simioni, M.: Adaptation of Rice Yields to Heat Stress in Vietnam: New Insight from Heterogeneous Slopes Panel Data Modeling. (2022). <https://hal.inrae.fr/hal-03715498> Accessed 2024-09-11
- World Bank Group, Asian Development Bank: Climate Risk Country Profile: Vietnam. World Bank, ??? (2021). <https://doi.org/10.1596/36367>
- World Meteorological Organization: The Global Climate 2011-2020: A decade of acceleration. Technical report, World Meteorological Organization (November 2023). <https://wmo.int/publication-series/global-climate-2011-2020-decade-of-acceleration> Accessed 2024-04-12
- World Meteorological Organization: State of the Global Climate 2023. Technical Report WMO-No. 1347, World Meteorological Organization (March 2024). <https://wmo.int/publication-series/state-of-global-climate-2023> Accessed 2024-04-12
- Zhang, J.-T., Chen, J.: Statistical inferences for functional data. *The Annals of Statistics* **35**(3), 1052–1079 (2007) <https://doi.org/10.1214/009053606000001505> . Publisher: Institute of Mathematical Statistics. Accessed 2025-02-11
- Zhang, J.-T., Cheng, M.-Y., Wu, H.-T., Zhou, B.: A new test for functional one-way ANOVA with applications to ischemic heart screening. *Computational Statistics & Data Analysis* **132**, 3–17 (2019) <https://doi.org/10.1016/j.csda.2018.05.004>
- Zhang, J.-T.: Statistical inferences for linear models with functional responses. *Statistica Sinica* **21**(3), 1431–1451 (2011) <https://doi.org/10.5705/ss.2009.302> . Accessed 2024-11-19
- Zhang, J.-T.: Analysis of Variance for Functional

1025 Data, 0 edn. Chapman and Hall/CRC, ???
1026 (2013). <https://doi.org/10.1201/b15005>

1027 Zhang, J.-T., Liang, X.: One-Way ANOVA for
1028 Functional Data via Globalizing the Point-
1029 wise F-test. Scandinavian Journal of Statistics
1030 **41**(1), 51–71 (2014) [https://doi.org/10.1111/](https://doi.org/10.1111/sjos.12025)
1031 [sjos.12025](https://doi.org/10.1111/sjos.12025)